Journal of Catalysis **185,** 23–32 (1999)
Article ID jcat.1999.2488, available online at http://www.idealibrary.com on IDEAL®

A Computer Simulation Study on Acylation Reaction of Aromatic Hydrocarbons over Acidic Zeolites

A. Chatterjee,*,[1] D. Bhattacharya,† T. Iwasaki,* and T. Ebina*

*Inorganic Material Section, Tohoku National Industrial Research Institute, 4-2-1 Nigatake, Miyagino-ku, Sendai 983-8551, Japan; and †Catalysis Unit, Department of Chemical Engineering, University of Cape Town, Rondebosch-7700, Cape Town, South Africa

Received July 10, 1998; revised February 2, 1999; accepted March 15, 1999

In the case of acylation reaction of aromatic hydrocarbons it is observed that acylation of toluene and naphthalene in the presence of acidic zeolites such as H–ZSM-5, H–ZSM-12, H–Beta, H–Mordenite, and H–Y results in different products with variable selectivities. It is observed experimentally that benzoylation of toluene and naphthalene over zeolite H–Beta follows the selectivity order: 4-methylbenzophenone > 2-methylbenzophenone > 3-methylbenzophenone and 2-benzoylnaphthalene > 1-benzoylnaphthalene, respectively. Zeolite H–Beta shows the best selectivity among all other acidic zeolites. To explain this selectivity order a computer simulation study has been performed. Molecular mechanics were used to calculate the individual strain, dimensions of reactant, and product molecules; the dimensions of zeolite cages were compared. The results show that zeolite Beta is the best zeolite in terms of fitting of the reactant and product molecules. DFT was applied to study the electronic property and interaction energy of reactant and product molecules with acidic zeolite framework to rationalize the mechanism of acylation reaction over acidic zeolites. Molecular electrostatic potential maps were also plotted from DFT to rationalize the polarization of the reactants in the reaction process. The results were compared with experimental observation which justifies the role of acidic zeolites, in this particular reaction.

INTRODUCTION

Selective benzoylation of toluene and naphthalene to 4-methylbenzophenone (4-MBP) and 2-benzoylnaphthalene (2-BON) is of considerable interest due to its commercial importance in the perfumery, dyes, and pesticides industries (1, 2). Due to their shape selectivity, thermostability, the easy separation from the products, and the possibility of regeneration of the deactivated catalysts, zeolites have been used widely in the field of organic fine chemical synthesis. In our previous communications (3, 4) we showed that compared to other acidic zeolites such as H–ZSM-5, H–ZSM-12, H–Beta, H–Mordenite, and H–Y, H–Beta produced selectively 4-MBP and 2-BON during the benzoylation of toluene and naphthalene, respectively, using benzoylchloride as the benzoylating agent. Although para-substitution generally predominates in classical Friedel–Crafts acylation, the exclusive formation of the para-isomers is rare and can only be explained by the shape selectivity of zeolites during product formation. Zeolite Beta is developing into a major catalyst in organic chemical conversion, contributing to low waste technology. In comparison with other zeolites, zeolite Beta possesses unique acid properties, which are related to local defects. These defects are generated when a tertiary building unit (TBU) is rotated 90° around the *c*-direction with respect to the neighboring TBUs in the same layer. The rotated TBU connects properly with the adjacent layers. This results in T-atoms that are not fully coordinated to the framework, thereby creating potential Lewis acid site (5). The valuable catalytic and reactive properties of zeolites provide ample reason for establishing a firm theoretical understanding of their structure and behavior. Computer simulation studies can contribute significantly in achieving an understanding of the structure property relationship by the synthesis of current understanding and data, revealing critical conceptual issues whose resolution demands additional experimentation. There has been a phenomenal growth of interest in theoretical simulations over the past decade and there have been some outstanding reviews in this field in the past couple of years (6–9). In our earlier study (10) we applied computer simulation techniques based on molecular mechanics and semi-empirical quantum chemical calculations to establish structural relations between the spirolactones and the zeolite voids, which otherwise need to be determined by tedious experimental studies. Our DFT results (11) validate the mechanism of the said reaction by studying the interaction of reactant and product molecules with the zeolite framework cluster model. In the present study, we try to explain our experimental observation of product selectivity for the benzoylation of toluene and naphthalene using computer simulation. Initially, the shape selective catalytic behavior of the zeolites is rationalized by comparing the dimension of the molecules and zeolite pore diameter using molecular mechanics. The

[1] To whom correspondence should be addressed.

0021-9517/99 $30.00

best zeolite in terms of shape selectivity was chosen. This was followed by force field calculations to determine the total strain energy of the reactant and product molecules. Then, the mechanism of interaction of reactant and product molecules with zeolite framework cluster models in general was studied by density functional quantum chemical calculations. The interaction energy between the organic molecules (reactant and product) and zeolite host lattice was studied to locate the reason for selectivity order and to validate the experimentally proposed mechanism of conversion reaction. The aim of the study is to correlate geometrical constraints in zeolites and adsorption energetics with observed yields and product selectivity, which is a step toward validating the experimental observation.

METHOD AND MODEL

The equilibrium geometry of the product molecules shown in Figs. 1a and 1b was obtained by force field calculations developed by Gelin and Karplus (12). The total strain energy of the molecule is expressed by the following equation,

$$E_{\text{total strain}} = E_{\text{bonded}} + E_{\text{non-bonded}}, \quad [1]$$

where

$$E_{\text{bonded}} = E_{\text{bond length}} + E_{\text{bond angle}} + E_{\text{dihedral angle}} + E_{\text{improper torsion}} \quad [2]$$

$$E_{\text{non-bonded}} = E_{\text{electrostatic}} + E_{\text{Van der Waals}} \quad [3]$$

The respective expressions used to calculate the individual terms are given elsewhere (13). The visualization and energy calculations were performed using the InsightII code of MSI, Inc. The strain energy of the molecule was minimized as a function of geometry by the steepest descent method to eliminate initial bad contacts and then later by the conjugate gradient and Newton–Raphson methods.

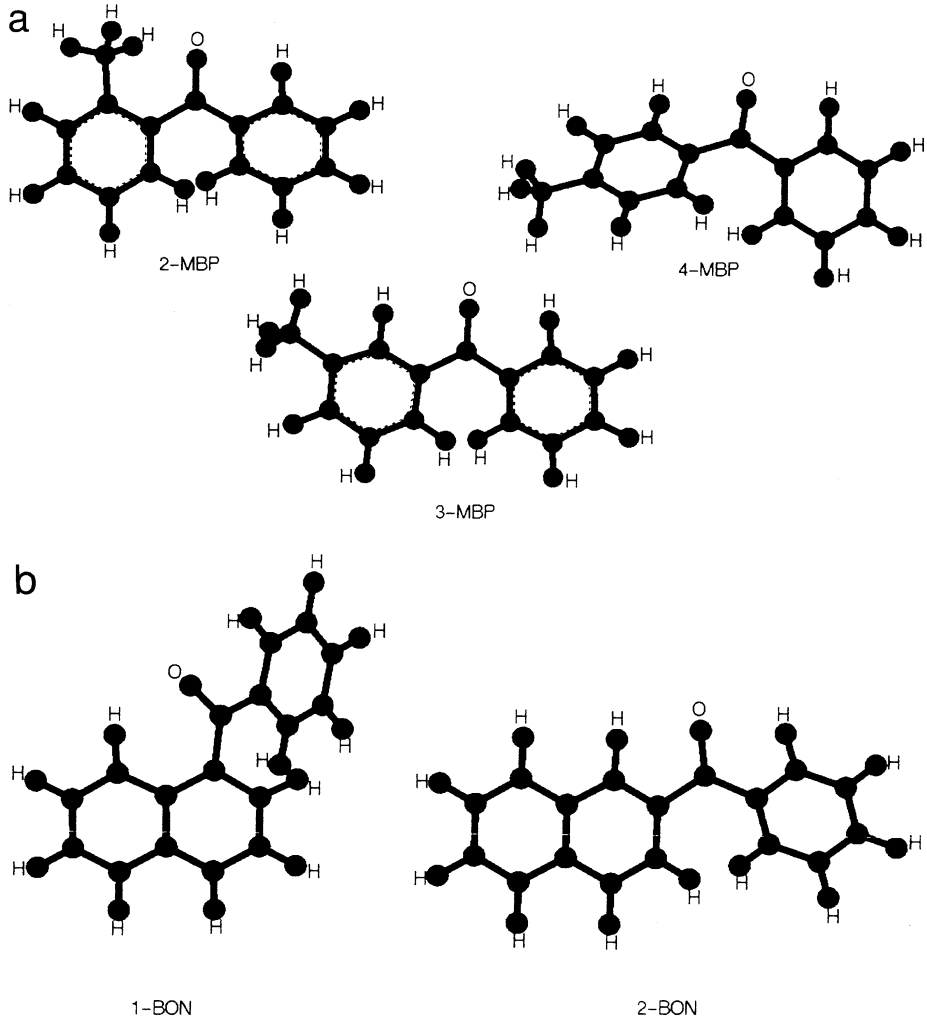

FIG. 1. (a) Optimized configuration of 2-MBP, 3-MBP, and 4-MBP using force field calculations. (b) Optimized configuration of 2-BON and 1-BON using force field calculations.

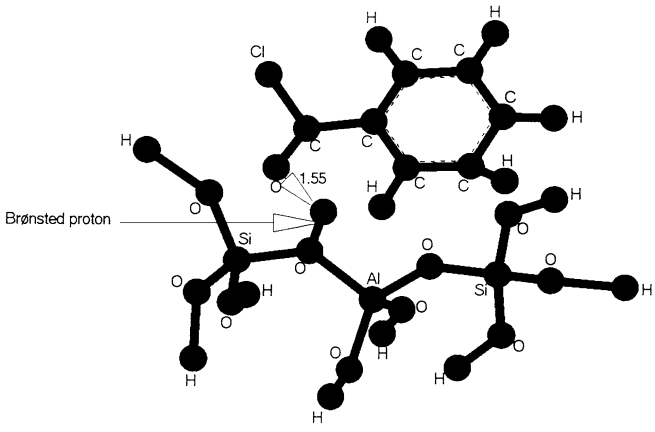

FIG. 2. Acidic zeolite framework cluster model with benzoyl chloride.

Nonlocal density functional (NLDF) calculations were performed using the DMOL program of MSI, Inc. (14) on a Silicon Graphics Indigo2 workstation. This approximation assumes that the electron density varies slowly in comparison to the exchange and correlation effects. A double numerical with polarization (DNP) basis set (15) with spin restricted energy calculations was performed with fine mesh grid and frozen core electrons. Because of the quality of these orbitals, basis set superposition effects (16) are minimized and an excellent description of an even weak bond is possible. A BLYP-type functional (17) was used for the exchange correlation energy terms in the total energy expression. The final geometries were accepted when the norm of the energy gradient was less than 0.002 au. At the optimized structure nonlocal functions were used to get the energy at the self-consistent level. Basis set superposition error was also calculated for the current basis set in nonlocal density approximation using the Boys–Bernardi method (18). The value is 3.45 kcal/mol. The molecular electrostatic potential (MESP) calculated by NLDF at given point r in space represents a first order approximation to the molecular charge distribution with the probe of unit charge at that point. The methodology has been described elsewhere (19).

We consider the cluster model of the formula $(HO)_3Si$–OH–Al–$(OH)_2$–O–$Si(OH)_3$ for the calculations. This model is a replica of the acid site of zeolite, which can interact with the reactant molecule. Hydrogen atoms are necessary to maintain the cluster neutrality for a substituted situation which was located at 1 Å along the bond axes connecting the bridging oxygen. The cluster model, along with benzoyl chloride, is shown in Fig. 2. The coordinates of the terminal hydrogens of the clusters are fixed throughout the calculation.

RESULTS AND DISCUSSION

Scheme 1 shows the products formed in the benzoylation of both toluene and naphthalene using benzoylchloride as the benzoylating agent. The liquid phase benzoylation of toluene with benzoylchloride has been studied over various acidic zeolites at 383 K. Zeolite Beta selectively produces 4-MBP over 3- and 2-methylbenzophenone (3-MBP and 2-MBP) (3), whereas liquid phase benzoylation of naphthalene over the same set of zeolites in the temperature range 333–358 K using benzoyl chloride shows the superiority of zeolite Beta in the selective production of 2-BON over 1-benzoylnaphthalene (1-BON) (4). Experimental results (3, 4) summarizing benzoylation results over different catalysts were tabulated in Tables 1 and 2, respectively. Now, although para-substitution predominates in classical acylation, the exclusive formation of para-isomers is rare and can only be explained by the shape selectivity of zeolites during product formation. The ortho-isomer for the benzoylation of toluene and more bulky 1-BON for the benzoylation of naphthalene would require a greater volume than the space available within the channels or cavities of the catalyst. The results show that (Table 1) H–Beta acts as the best zeolite in terms of product selectivity and the product selectivity is in the order 4-MBP > 3-MBP > 2-MBP. Similarly the results shown in Table 2 indicate H–Beta as the best candidate for benzoylation of naphthalene and the product selectivity is in the order 2-BON > 1-BON. To justify the product selectivity the product molecules were minimized using a force-field procedure, and to explain the mechanism the interaction energy of molecules with a zeolite framework cluster containing an acid site was monitored.

Force Field Calculations

The three-dimensional equilibrium conformations corresponding to the minimum strain energy were obtained with a well-established force field (12) and their realistic three-dimensional conformations are shown in Figs. 1a and 1b. The respective strain energy values are included in Table 3. The analysis of the individual contributions of various bonded and nonbonded terms to the strain energy of these molecules was discussed in our earlier report (20).

TABLE 1

Benzoylation of Toluene over Different Zeolites

Catalyst	Time (h)	Conv. of BOC (wt%)	Activity (mmol/g/h)	Product selectivity (wt%) 2-MBP	3-MBP	4-MBP
H–ZSM-5	18	4.2	0.6	14.6	5.1	80.3
H–ZSM-12	18	41.0	6.7	2.4	2.9	94.7
H–Beta	18	83.4	9.9	3.4	1.3	95.3
H–Mordenite	18	19.5	2.0	14.9	4.4	80.7
H–Y	18	18.8	1.9	22.9	6.1	71.0
$AlCl_3$	1	67.3	14.5	22.0	3.9	74.1
SiO_2–Al_2O_3	18	1.8	0.4	25.4	3.4	71.2

Note. Reaction conditions: catalyst/C_6H_5COCl (w/w) = 0.33, reaction temperature = 383 K, Toluene/C_6H_5COCl (mol/mol) = 5, toluene = 0.11 mol. 2-MBP, 2-methylbenzophenone; 3-MBP, 3-methylbenzophenone; and 4-MBP, 4-methylbenzophenone.

TABLE 2

Benzoylation of Naphthalene with Benzoylchloride

Catalyst	Time (h)	Conv. of BOC (wt%)	Initial rate	Product selectivity (wt%)			2-BON/ 1-BON
				1-BON	2-BON	Others	
H–RE–Y	1	0.2	0.05	62.6	25.4	12.0	0.40
	18	7.2	—	59.8	20.0	20.2	0.33
H–Beta	1	1.5	0.36	17.9	82.1	—	4.58
	18	17.6	—	17.4	74.8	7.8	4.30
$AlCl_3$	1	14.6	3.52	87.3	7.2	5.5	0.08
H–ZSM-5	18	—	—	—	—	—	—

Note. Reaction conditions: catalyst/BOC = 0.37 (w/w), Naphthalene/BOC (mol./mol) = 2, Naphthalene = 0.039 mol, 1,2 dichloroethane = 15 g, reaction temperature = 358 K. 1-BON, 1-benzoylnaphthalene; 2-BON, 2-benzoylnaphthalene; others, dibenzoylnaphthalene.

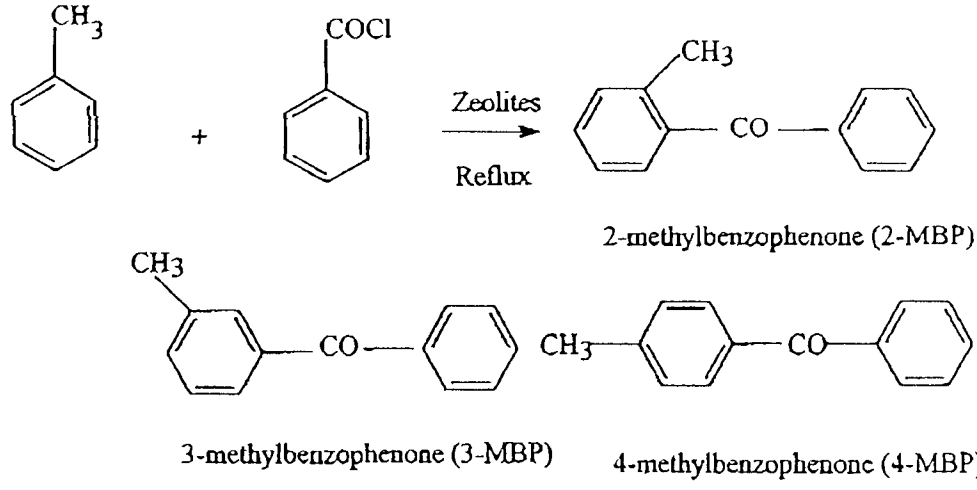

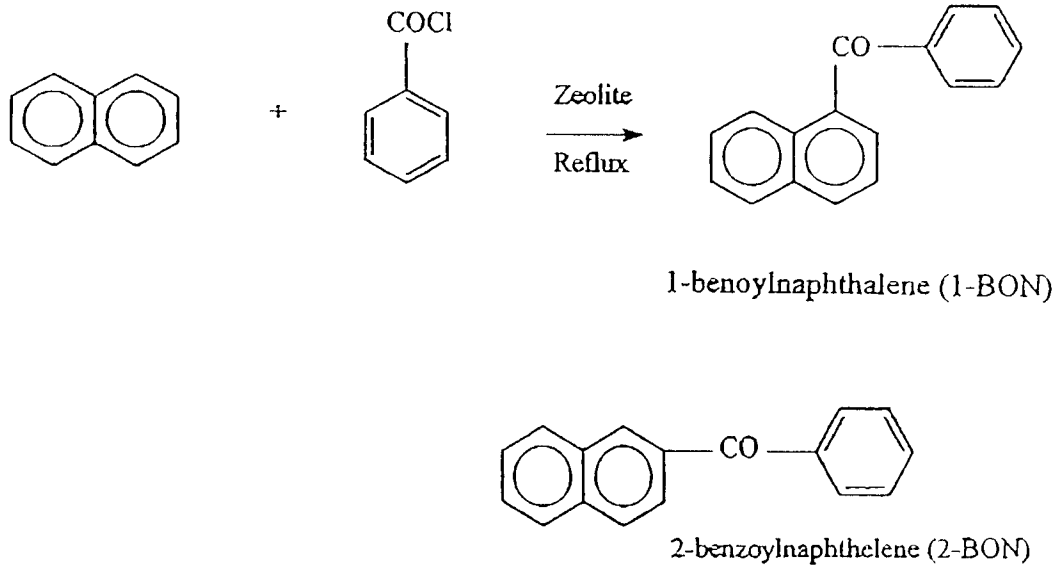

SCHEME 1. Product formation in both benzoylation of toluene and naphthalene using benzoylchloride as benzoylating agent.

TABLE 3

Force Field Calculation Results for the Product Molecules

Molecule	Total nonbond strain energy (kcal/mol)	Total electrostatic strain energy (kcal/mol)	Total bond strain energy (kcal/mol)	Total strain energy (kcal/mol)
2-MBP	1870.65	312.69	507.09	2655.39
3-MBP	1665.04	115.53	481.50	2347.77
4-MBP	1602.23	58.57	481.50	2291.04
2-BON	2325.40	163.96	744.16	3241.36
1-BON	2341.42	250.20	704.26	3478.42

Nonbonded energy arises from electrostatic and Van der Waals interactions. Favorable and unfavorable nonbonded terms arise due to the attraction between polar groups with unlike charges and the repulsion between polar groups with like charges, respectively. Here we observe that both bonded and nonbonded strain energy is unfavorable as indicated by the positive value, but the order decreases according to the order of selectivity observed experimentally. The unfavorable nonbonded energy for product molecules indicates the presence of positively charged groups in the molecule. These results indicate the positive charges in the molecules have ionic interaction with the basic oxygen of the zeolite framework, which could lead to their mode of adsorption inside the zeolite void volume. The product yields with various zeolite catalysts are in correspondence with their structural fitting. It can be generalized that large pore zeolites with cage structures are efficient catalysts for the acylation reaction. Thus the role of shape selectivity in controlling the yield is commonly brought out from these results.

The Importance of the Void Dimensions in Zeolites

Breck (21) had initiated a convention of reporting the kinetic diameter of a molecule as the intermolecular distance at the closest approach of two molecules. Recently, there have been phenomenal advances in molecular graphics techniques. Hence, more accurate information regarding the size, namely the three largest dimensions of the molecules, could be provided. The methodology was discussed in our earlier article (22). Assuming that a molecule fits exactly inside the smallest possible rectangular box, then the dimensions of the molecule are the dimensions of the box. The three largest dimensions of a molecule, therefore, are *a* (length), *b* (breadth), and *c* (width). This will be compared with the size of the pore openings or diameters of the channels of the zeolites. The pore diameters of various zeolites are known from the reported crystal structure (23). It is possible to study the fitting of different product molecules in the various zeolites used to predict the shape selectivity. Now the reactant toluene and naphthalene can enter the zeolite cages and can hop around the cage, but the product dimensions seem to be crucial for this reaction. These results are illustrated in Figs. 3 and 4 for products generated from toluene and naphthalene, respectively. The order of

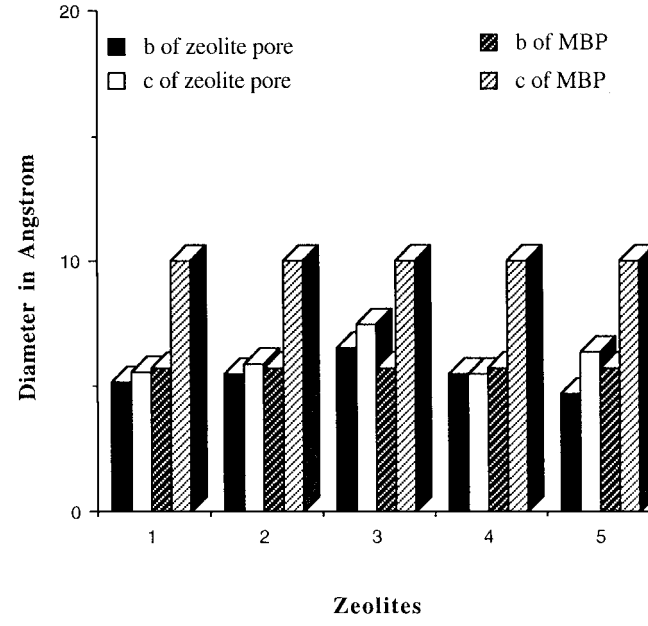

FIG. 3. The schematic representation of pore diameters in various zeolites used as catalysts (order follows that of Table 1). The range of two average dimensions (*b*, *c*) of methylbenzophenones (MBP) was compared with the average diameters of the pore openings of the zeolites.

FIG. 4. The schematic representation of pore diameters in various zeolites used as catalysts (order follows that of Table 1). The range of two average dimensions (*b*, *c*) of benzoylnaphthalenes (BON) was compared with the average diameter of the pore openings of the zeolites.

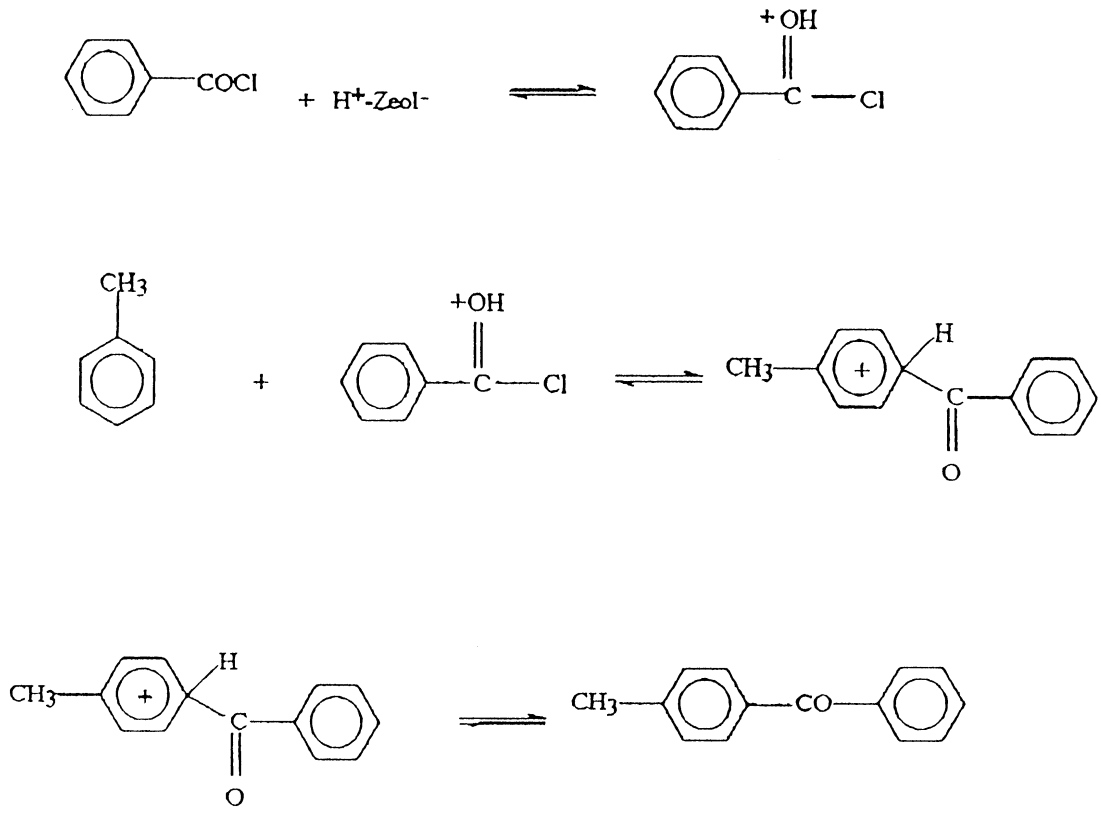

SCHEME 2. General mechanism of Friedel–Crafts acylation over zeolites as proposed by Corma *et al.* (24).

zeolites mentioned in the *x*-axis follow Table 1. For both reactions five zeolites were compared. The results show the superiority of zeolite Beta in terms of shape selectivity qualitatively. Now the largest dimension can be neglected (*a*), as it is the length of the molecule which lies along the axis of the channel; the other two dimensions (*b*, *c*) are important, which dictates the fitting of the molecule inside the zeolite pore.

Importance of Interaction Energy

Although the void dimensions of the zeolite catalysts control the product yield, the electronic interactions are also expected to play a vital role in the mechanism of this reaction. Corma *et al.* (24) proposed the general mechanism of the Friedel–Crafts acylation over zeolites as shown in Scheme 2. According to this mechanism, the Brønsted acid sites react with the acylating agent to produce an acylium ion or an acylium-like complex. The electrophilic species generated through this interaction, attack the aromatic ring in the second step to form a metastable complex, which after abstraction of a hydrogen cation transformed into the product. The nature of the product formed depends on the attacking position of the electrophile on substituted aromatic ring. As there is not much difference in the dimensions of the product molecules the selectivity can be accounted for by using the interaction energy calculations using DFT. The electronic properties of toluene, naphthalene, benzoylchloride (acylating agent), the framework cluster, and all the product molecules were calculated by full geometric optimization using DFT. The results are shown in Table 4. Then we follow the proposed reaction Scheme 2 for calculating the interaction energy through a hypothetical transition state by varying only the distance parameter. In terms of the framework cluster the reaction steps were as

TABLE 4

Electronic Properties of Framework Cluster, Reactant, and Product Molecules as Calculated by DFT

Molecules	Total energy (kcal/mol)
Benzoylchloride	−502554.2
Toluene	−456387.1
Naphthalene	−240005.1
Framework cluster	−985383.9
2-MBP	−383201.1
3-MBP	−383201.3
4-MBP	−383201.5
2-BON	−454325.6
1-BON	−454326.2

follows:

1st step:

$$C_6H_5COCl + ZeolOH \rightarrow [ZeolO^-C_6H_5COHCl^+]$$

2nd step (metastable intermediate):

$$[ZeolO^-C_6H_5COHCl^+] + C_6H_5CH_3 \rightarrow C_6H_5COHC_6H_5CH_3ZeolO^- + HCl$$

from which the final product is generated: $C_6H_5COC_6H_5CH_3$.

First we calculated the interaction energy by manually changing the distance between the Brønsted proton of the zeolite framework and the C=O of the acylating agent to locate the hypothetical transition state for proton abstraction. Then we calculated the interaction energy which resulted when toluene and naphthalene interacted with the zeolite framework. This was followed by the calculation of the interaction energy for individual products with zeolite clusters to compare the product selectivity. The metastable intermediate was not tested. Now, the maximum instability resulting from the reaction with toluene will show the activity of the zeolite while the stability of the product inside the zeolite framework will explain its respective selectivity.

Table 5 shows the results of proton abstraction from zeolites. Now, the distances between oxygen of the C=O moiety of C_6H_5COCl and the Brønsted proton of zeolite were varied and the stabilization energy for each distance was monitored. The aim was to compare the experimental prediction about proton abstraction and in the process to validate our model. The results show that at a distance of 1.55 Å between the Brønsted proton and the C=O of C_6H_5COCl the complex became stabilized or in some other way the interaction energy is most favorable. We optimize the full structure with a constraint on the terminal hydrogens at every distance. We get potential minima at the said distance; anything more or less than the distance causes instability. So we choose this configuration as the first step of the reaction as shown in Scheme 2. This is followed by the interaction energy calculation with $[C_6H_5COHCl^+]$, toluene, or naphthalene inside the zeolite framework from which the Brønsted proton was already abstracted. In this situation the complex neutrality is there whereas the zeolite framework is having a total charge of −1 interacting with unipositive $[C_6H_5COHCl^+]$. This is a model to replicate the reaction inside the zeolite cage. The results were shown in Table 6. It is observed that 4-MBP and 2-BON are the most unstable among the three isomers (2-MBP, 3-MBP, and 4-MBP) and two isomers (2-BON and 1-BON) for the benzoylation of toluene and naphthalene, respectively. This is a calculation to validate the reaction path (Scheme 2). As it is difficult to perform the calculation for a metastable intermediate, we performed this interaction of a complex with zeolite framework (proton abstracted), which shows the instability in terms of interaction energy which further dictates the possibility of elimination of hydrogen to generate the respective product molecules. The model is shown in Fig. 5. This is followed by the calculation for the product interaction with the zeolite framework cluster, which will further validate the shape selectivity order in the case of acidic zeolites.

TABLE 5

Interaction Energy as a Function of Distance between the Brønsted Proton of the Zeolite Framework Cluster and C=O of C_6H_5COCl as Calculated by DFT

Distance (in Å)	Total energy (kcal/mol)	Interaction energy (kcal/mol)
1.35	−1487968.5	−25.7
1.55	−1487963.9	−30.3
1.67	−1487960.7	−22.5
1.83	−1487962.8	−24.6

TABLE 6

Interaction Energy of $[C_6H_5COHCl^+]$ and Toluene or Naphthalene (as the Case May Be) with Zeolite Framework Cluster from Which the Proton Is Already Abstracted by DFT

Product to be formed	Total energy (kcal/mol)	Interaction energy (kcal/mol)
2-MBP	−1368631.7	−46.6
3-MBP	−1368623.5	−38.2
4-MBP	−1368611.2	−25.7
2-BON	−1439785.2	−75.6
1-BON	−1439802.4	−92.1

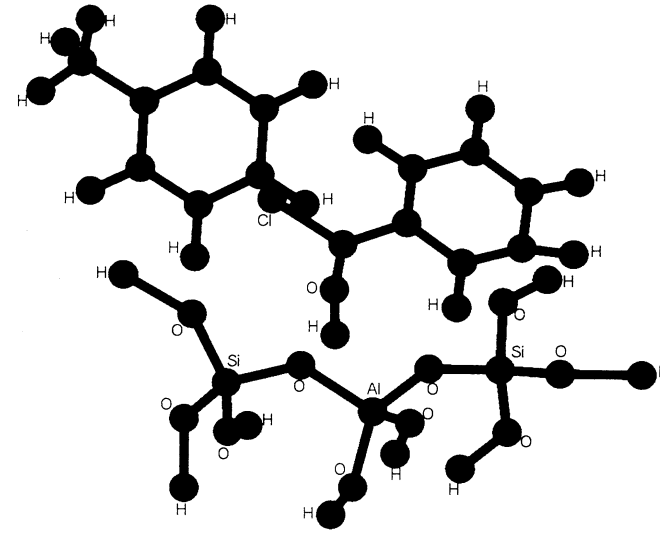

FIG. 5. Toluene interacts with benzoylcloride and the zeolite framework cluster model (proton abstracted).

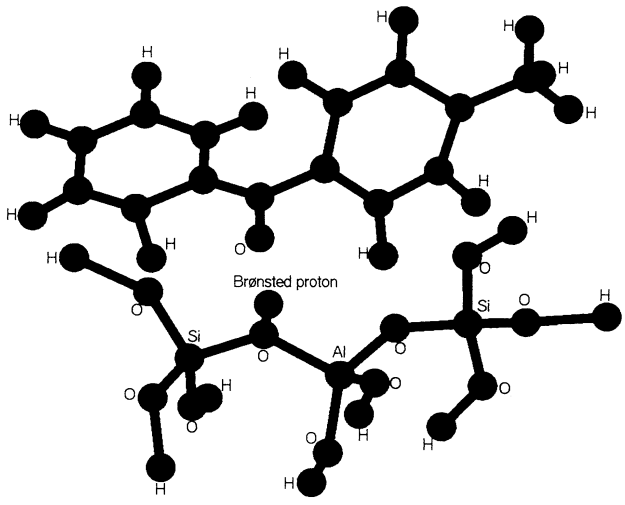

FIG. 6. 4-MBP interacts with the zeolite framework cluster model.

The model is shown in Fig. 6. The results are tabulated in Table 7. Now these energies are significantly higher than those expected (60 KJ/mol) from single hydrogen bonds between carbonyl oxygen atoms and acidic hydroxyl groups on oxide surfaces (25, 26). This can be explained in terms of the fact that the reaction is taking place inside the zeolite cage, so the environment of the Brønsted proton really matters. In the case of zeolites, the acidic proton has a bridging oxygen linked with Si terminated by hydrogens which results in a steep increase in the energy value, as also observed by other researchers in this field (27, 28). The results show that the order of stability is less for product molecules having higher selectivity. The order obtained from the interaction of product molecules with a zeolite cage shows the order 4-MBP > 3-MBP > 2-MBP for the acylation reaction of toluene, whereas the product of acylation reaction of naphthalene shows the order of 2-BON > 1-BON. We then compared this order with experimental observation to assimilate the power of computer simulation. Although this interaction energy calculation cannot predict the actual mechanism, the path can be compared with the experiment qualitatively. In all the cases BSSE correction is included and accounted for. The results are in an excellent match with experimental order.

MESP Map

The MESP was plotted for a potential range of −0.05 a.u. +0.05 au. The results were shown for proton abstraction during the interaction of benzoylchloride with the framework (Fig. 7) and for the interaction of product 2-BON with the zeolite framework (Fig. 8). It is observed from Fig. 7 that the strong negative potential around C=O pulls the Brønsted proton having high positive potential which then results in the abstraction of the proton. This validates Scheme 2 where the first step is a proton abstraction resulting in an acylium ion. Now, for product interaction Fig. 8 shows the elimination of hydrogen back to the basic oxygen site of zeolite framework resulting from the mutual attraction of the positive and negative potential. MESP shows the region of plausible bond breaking and bond formation, which may further help in the future study of locating the transition state. MESP thus shows the proton abstraction form framework as well as hydrogen atom elimination from the intermediate to form the product. This also supports the reaction mechanism proposed by the experiment.

TABLE 7

Interaction Energy for Product Molecules with a Zeolite Framework Cluster by DFT

Molecules	Total energy (kcal/mol)	Total energy (kcal/mol)
2-MBP	−1944363.9	−31.2
3-MBP	−1944354.2	−24.6
4-MBP	−1944337.5	−12.2
2-BON	−1727943.3	−58.6
1-BON	−1727967.8	−73.2

CONCLUSION

The shape selective catalytic behavior of various zeolites has been rationalized. The structural fitting of the product molecules whose selectivity was to be tested was compared in terms of strain energy by force field calculations and then the fitting of these molecules inside all the five zeolite cages has been tested to show the superiority of zeolite Beta. This acylation reaction can only be done with acidic zeolite, so to understand the reason for product selectivity and the role of acidic zeolite in general, density functional calculations were performed. The mechanism proposed by the experiment was followed throughout the calculation. The results were further supported by MESP. The results justifies the order for benzoylation of toluene to produce three isomers with the selectivity order 4-MBP > 3-MBP > 2-MBP and for benzoylation of naphthalene the selectivity order for the

FIG. 7. MESP for benzoylchloride interacting with the zeolite framework. The +ve (+0.05 to 0.00 au.) and −ve (−0.05 to 0.00 au.) potential contours are shown as green and red shades respectively.

FIG. 8. MESP for 4-MBP interacting with zeolite framework. The +ve (+0.05 to 0.00 au.) and −ve (−0.05 to 0.00 au.) potential contours are shown as green and red shades, respectively.

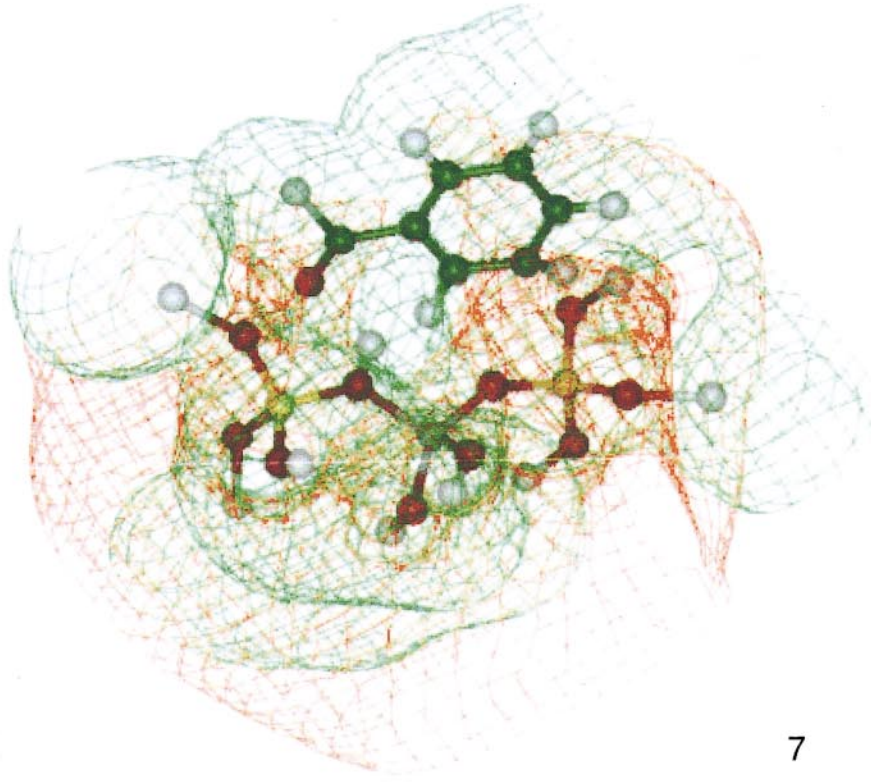

7

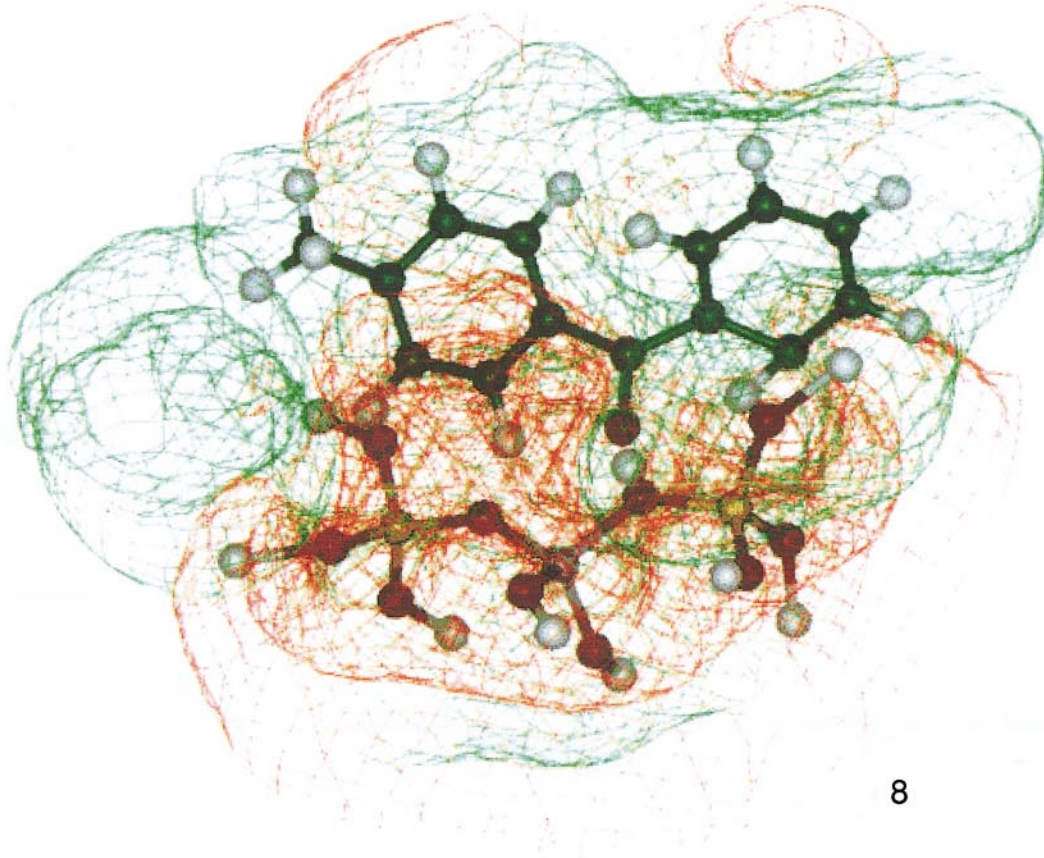

8

two isomers is 2-BON > 1-BON. The molecular mechanics help to test the fitting and then DFT traces the reaction path. It shows the bond cleavage and bond formation in the acylation reaction of aromatic hydrocarbons. The applicability of computer simulation studies has been established in this reaction and can be extrapolated to any such chemical reaction in zeolite matrices.

REFERENCES

1. Fieser, L. F., and Feiser, M., *in* "Organic Chemistry," p. 915. Asia Publishing, New Delhi, 1965.
2. Hammand, H. A., Doty, J. C., Laakso, T. M., and Wiliams, J. L. R., *Macromolecules* **3**, 711 (1970).
3. Singh, A. P., Bhattacharya, D., and Sharma, S., *J. Mol. Catal.* **102**, 139 (1995).
4. Bhattacharya, D., Sharma, S., and Singh, A. P., *Appl. Catal.* **150**, 53 (1997).
5. Jansen, J. C., Creyghton, E. J., Njo, S. L., Koningsveld, H. V., and Bekkum, H. V., *Catal. Today* **38**, 205 (1997).
6. Bates, S. P., and van Santen, R. A., *Adv. Catal.* **42**, 1 (1998).
7. Haw, J. F., and Xu, T., *Adv. Catal.* **42**, 115 (1998).
8. Sauer, J., Ugliengo, P., Garrone, E., and Saunders, V. R., *Chem. Rev.* **95**, 637 (1995).
9. Sauer, J., *Chem. Rev.* **89**, 199 (1989).
10. Chatterjee, A., Vetrivel, R., Sreekumar, R., Murthy, Y. V. S. N., and Pillai, C. N., *J. Mol. Catal. A* **127**, 153 (1997).
11. Chatterjee, A., Iwasaki, T., Ebina, T., and Vetrivel, R., *J. Mol. Graphics Mod.* **15**, 215 (1998).
12. Gelin, B. R., and Karplus, M., *Biochemistry* **18**, 1265 (1979).
13. Bhawal, B. M., Vetrivel, R., Reddy, T. I., Deshmukh, A. R. A. S., and Rajappa, S., *J. Phys. Org. Chem.* **7**, 377 (1994).
14. Kohn, W., and Sham, L. J., *Phys. Rev. A* **140**, 1133 (1995).
15. Delly, B. J., *J. Chem. Phys.* **94**, 7245 (1991).
16. Delly, B. J., *J. Chem. Phys.* **92**, 508 (1990).
17. Lee, C., Yang, W., and Parr, R. G., *Phys. Rev. B* **37**, 786 (1988).
18. Boys, S. F., and Bernardi, F., *Mol. Phys.* **19**, 553 (1970).
19. Vetrivel, R., Deka, R. C., Chatterjee, A., Kubo, M., Broclawik, E., and Miyamoto, A., *Theor. Comp. Chem.* **3**, 509 (1996).
20. Chatterjee, A., Vetrivel, R., Sreekumar, R., Murthy, Y. V. S. N., and Pillai, C. N., *in* "Catalysis: Modern Trends" (N. M. Gupta, and D. K. Chakraborty, Eds.), p. 68. Narosa Publishing, New Delhi, 1996.
21. Breck, D. W., *in* "Zeolite Molecular Sieves: Structure, Chemistry and Use," p. 634. Wiley, New York, 1974.
22. Chatterjee, A., and Vetrivel, R., *J. Chem. Soc. Faraday Trans.* **91**, 4313 (1995).
23. Meier, W. M., and Olson, D. H., *in* "Atlas of Zeolite Structure Types, Zeolites," Butterworth-Heinman, London, 1992.
24. Corma, A., Climent, M. J., Garcia, H., and Primo, P., *Appl. Catal.* **49**, 109 (1989).
25. Hertl, W., and Hair, M. L., *J. Phys. Chem.* **72**, 4676 (1968).
26. Allian, M., Borello, E., Ugliengo, P., Spano, G., and Garrone, E., *Langmuir* **11**, 4811 (1995).
27. Van Santen, R. A., and Kramer, G. J., *Chem. Rev.* **95**, 637 (1995).
28. Kramer, G. J., and van Santen, R. A., *J. Am. Chem. Soc.* **115**, 4811 (1993).